Review of Spectral Indices for Urban Remote Sensing

Akib Javed, Qimin Cheng, Hao Peng, Orhan Altan, Yan Li, Iffat Ara, Enamul Huq, Yeamin Ali, and Nayyer Saleem

Abstract

Urban spectral indices have made promising improvements in the last two decades in urban land use land cover studies through mapping, estimation, change detection, time-series analyzing, urban dynamics, monitoring, modeling, and so on. Remote sensing spectral indices are unsupervised, unbiased, rapid, scalable, and quantitative in information extraction. Hence, we aimed to summarize the most relevant urban spectral indices by focusing on multispectral, thermal, and nighttime lights indices. We use the search terms "urban index", "built-up index", "normalized difference built-up area (NDBI)", "impervious surface index", and "spectral urban index" to collect relevant literature from the "Web of Science Core Collection" database. We found that all urban spectral indices developed since 2003, except NDBI. This review will help understand the applications of urban spectral indices, the selection of indices based on available spectral bands, and their merits and demerits.

Introduction

Background

In urban remote sensing (RS), the last two decades produced numerous promising urban spectral indices for urban land use land cover (LULC) studies. RS applications are now fundamental, from urban planning to urban governance. Old maps and field surveys are outdated and rapidly replaced by RS images for urban studies (Li *et al.* 2018). From the mapping of a single city (Shao *et al.* 2019, Zhang *et al.* 2021), regional (Lyimo *et al.* 2020) to global land use mapping (Duan *et al.* 2015; Liu *et al.* 2018; Zhang and Seto 2011) are now possible with RS technology.

Earlier Remote Sensing Urban Studies

Earlier, RS or urban studies were focused on urban area mapping, urban land use classification, urban-rural fringe study, and urban heat islands (UHI) (Li *et al.* 2021, Shao *et al.* 2021). In the earliest quantitative techniques in urban change detection studies using RS images, urban and nonurban areas were delineated using the boundaries of vegetated and non-vegetated areas. This study also introduced the false-color composite by replacing earlier grayscale images (Howarth and Boasson 1983).

In digital image classification techniques, the importance of spectral characteristics (Digirolamo and Davies 1994; Vachon and West 1992) and spectral signature (Dekker *et al.* 1992; Surin and Ladner 1995) were also increased among other RS researchers since then.

In the beginning, band ratios were popular first, followed by normalized urban indices like normalized difference vegetation index (NDVI). Colwell (1974) first used a band ratio of near-infrared (NIR) and red bands for vegetation study from the Landsat multispectral scanner (MSS) sensor. Later, this ratio was popularized as a simple ratio (SR) (Baret *et al.* 1989; Sellers 1987). Afterward, the SR was normalized as vegetation index (VI) (Rouse Jr *et al.* 1974) and popularized later on as NDVI (Huete 1988). Unlike vegetation, urban indices primarily focused on short wave infrared (SWIR) and NIR spectral regions, where built-up areas reflect more in SWIR electromagnetic spectrum regions than the NIR region. Using this spectral information, urban index (UI) is one of the earlier examples of an urban index in urban RS studies (Kawamura *et al.* 1997).

Urban Indexing with Multispectral RS

Multispectral RS data sets have popularity among urban researchers because it has a medium spatial resolution, shorter temporal resolution, spectral resolution with visible NIR, SWIR, and thermal bands, available global coverage, easy accessibility, and so on. Among the major RS data sources, Landsat missions have the most extended stable historical archive of freely available remote sensing instruments (RSI) with global coverage among all the multispectral sensors, attracting researchers for time series analyses. *Sentinel-2A/B* also has a better spatial resolution than Landsat, with some visible bands up to 10 meters. On the other hand, moderate resolution imaging spectroradiometer (MODIS) has extensive coverage for regional studies but a very short temporal gap, attracting many regional studies with low spatial resolution requirements. A visible/infrared intelligent spectrometer (VIRIS) has better spectral resolution but is limited spatiotemporally. In this way, each RS sensor has its merits and demerits. Researchers have to design their research according to their data availability.

Urban Indexing with Cloud Computing

Computing platforms further widens the possibilities of many RS studies, including urban studies. Primarily, Google Earth Engine (GEE), enabling users to study large numbers of RSI (Gorelick *et al.* 2017; Shelestov *et al.* 2017) very quickly.

Akib Javed, Hao Peng, Enamul Huq, and Nayyer Saleem are with the State Key Laboratory of Information Engineering in Surveying, Mapping and Remote Sensing, Wuhan University, Wuhan, 430079 Hubei, China (akibjaved@whu.edu.cn).

Qimin Cheng is with the School of Electronics Information and Communications, Huazhong University of Science and Technology, Wuhan, Hubei 430074, China.

Orhan Altan is with the Department of Geomatics, Istanbul Technical University, Istanbul, Turkey.

Yan Li is with the Inner Mongolia Electronic Information Vocational Technical College, Hohhot 010070, China.

Iffat Ara is with the Department of Environmental Science and Geography, Islamic University, Kushtia 7003, Bangladesh.

Yeamin Ali is with DanChurchAid, Cox's Bazar, 4700, Bangladesh.

Contributed by Zhenfeng Shao, October 1, 2020 (sent for review November 16, 2020; reviewed by Bin Hu, Nana Yaw Danquah Twumasi, Neema S S Sumari)

Photogrammetric Engineering & Remote Sensing
Vol. 87, No. 7, July 2021, pp. 513–524.
0099-1112/21/513–524

doi: 10.14358/PERS.87.7.513

Furthermore, it increased computational capacity and sharing capability in many folds among researchers. These events triggered an RS big data study in spatial mapping, change detection, and time series analysis.

Indexing Urban Areas

Spectral Indexing for Urban Studies

Spectral indexing allows quantitative enhancement of RS information. Indexing facilitates urban RS studies by fusing multiple data sets, extracting objective information, automating image processing, avoiding researcher bias, easing scaling-up operation, bring robustness in RSI data analysis, and overall speeding-up of urban study.

Prior, unlike vegetation and water indexing, urban spectral indexing was uncommon. Almost all the indices were developed after 2000. Initially, urban indexing focused on broad urban characteristics where the concept of urban was considered a densely populated place. Subsequent, indices focused only on the infrastructural characteristics of an urban area.

Finally, the built-up area's impervious characteristics were emphasized in indexing as an urban indicator. Both the built-up area and impervious surface area (ISA) have spectral similarity with bare soil. Therefore, most of the indices with built-up areas consider it as a limitation. On the contrary, a bare soil area is pervious and, by definition, opposite of ISA. Therefore, researchers emphasized much in solving classification problems between bare soil area and ISA.

Index-Based Urban Classification

There are many urban area extraction methods in the RS domain. Spectral indices are one of them in pixel-level classifications. It is easy to apply in broad arrays of RS application than a traditional classification algorithm (Pan *et al.* 2010). Spectral indices provide a probability output with continuous value, where classifiers provide discrete values (Xie *et al.* 2008) in image classification. Therefore, in quantitative manipulations, indices are popular among researchers. Even in subpixel level classifications, indices are popular with spectral mixing analysis to derive endmembers (Li 2020).

Supervised image classification required sampling as training data and could not replicate across geographical variations accurately. In contrast, indexing-based classification is an unsupervised method, easy to replicate globally, can deal with big data sources, and has robust characteristics (Datta *et al.* 2008; Olaode *et al.* 2014). Therefore, spectral indices-based image classifications are becoming popular with various spatiotemporal studies due to their nonreliability on training data (Phalke and Özdoğan 2018).

Classification Problems in Urban Indexing

Spectral indices are useful for studying RSI, measuring LULC classes, and detecting changes of LULC over time. Urban land use classes are different from the rest of the land cover types where it is human-made land use, unlike other natural land covers (Meyer and Turner 1994). Secondly, urban areas are highly heterogeneous, fragmented, and mixed with other LULCs. Thirdly, its spectral signature is confusing where bright pixels have similarity with dry bare soil and dark pixels have high similarity with shadow, wet bare land, and shallow waterbodies.

Often urban ISA extraction requires removing nonurban classes (Khan *et al.* 2017). Furthermore, other land cover classes' spectral indexing can also refine urban classification accuracy by removing cloud coverage (Gomez-Chova *et al.* 2017), waterbodies (Deng and Wu 2012), and bare soil. Besides, urban built-up areas and bare soil areas have difficult classification problems in RS studies with existing multispectral data sets. We present an overview of spectral indices where few indices dealt with this problem. In addition to LULC studies, numerous environmental studies used urban spectral indices.

Spatial Resolution in Urban Studies

Urban land use is a mixed area with ISA, vegetation, waterbodies, and bare soil. Coarse spatial resolution RS data such as MODIS will have very skewed results. Higher spatial resolution, such as medium resolution RS, can effectively classify RS images into limited numbers of classes (Ridd 2007). Medium RS images with 10–30 meters spatial resolution are sufficient for mapping urban features, but not enough to map urban heterogeneity. Hence, Landsat missions or *Sentinel's 2A/B* missions are sufficient for urban study with limited accuracy.

Along with land cover mapping (Hester *et al.* 2010; Jawak and Luis 2013; Parent *et al.* 2015), high-resolution RS data have also been used for specific urban features studies, such as urban vegetation (Chikr El-Mezouar 2011; Nichol and Lee 2006), urban water stress (Wu *et al.* 2018), urban landscape evapotranspiration (Nouri *et al.* 2014), the building detection method (Qin and Fang 2014), the earthquake affected building collapse (Liu and Li 2019), and so on. Although, in this spatial resolution, there are several accuracy issues because of mixed pixel problems. RS methods, such as spectral unmixing, can further enhance accuracy at the subpixel level.

Simple to Complex Urban Indexing

Generally, complexity in index formulation is positively related to accuracy and negatively related to robustness. Simple indices are robust to use but lack accuracy, whereas complex indices are more accurate but require more RS information. Often, this lack of RS information (i.e., spectral bands) makes complex indices unusable.

For example, vegetation temperature light index (VTLI) (Hao *et al.* 2015) and modified normalized difference impervious surface index ($MNDISI_{Liu}$) (Liu *et al.* 2013) both provide higher accuracy in comparison with simple normalized difference built-up index (NDBI) (Zha *et al.* 2003) but require multispectral, thermal, and nighttime lights (NTL) RS information to be formulated. While studying time series analysis, researchers were trying to use simpler indices so that these indices are calculatable with available RS data (Capolupo *et al.* 2020).

Significance of the Study

Among major LULC classes, vegetation has a couple of reviews articles with spectral indices (Kobayashi *et al.* 2019; Xue and Su 2017). On the contrary, there is a shortage of review works on urban spectral indexing. Besides, there are many urban indices developed and published in the last two decades. This review will try to compile most of the important spectral indices used in urban studies and categorize them. We used the "Web of Science" database and searched for terms "urban index", "urban spectral index", "normalized difference built-up index", "impervious surface area", and a combination of these terms, which found a total of 1447 articles within the English language (Figure 1).

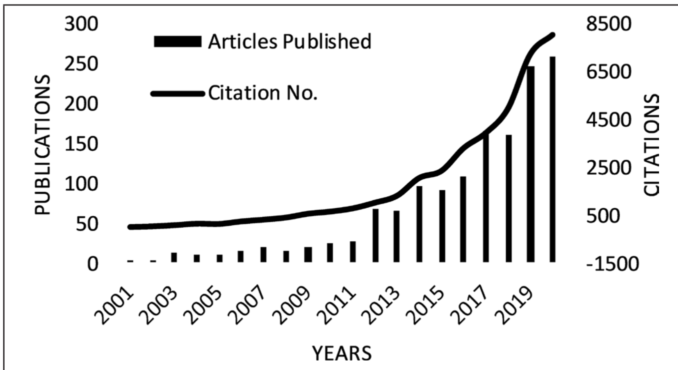

Figure 1. Bar graph shows yearly publications count and the line graph shows citation count for urban-related spectral indices. The search was conducted on 9 January 2021. Only article literature are included.

This review summarizes the most used, popular, and important urban spectral indices from multispectral, thermal, and nighttime lights RSI. We also classify them according to their band usage.

In those segments, we discuss their applicability, merits and demerits, and their band equations. This study will support researchers studying urban indexing, spectral indexing, and urban spectral indices. It will assist in understanding the overall picture of the topic and development phases of urban indices.

Spectral Urban Indexing

Urban indexing began with infrared spectral bands. These earlier indices were inefficient and built-up areas were mixed with bare soil. Therefore, new indices were developed using different bands, such as panchromatic (PAN), coastal, thermal bands, etc. Later on, complex transformations such as tasselled cap transformation (TCT), principal component analysis (PCA), and NTL were introduced to enhance accuracy. However, the focus shifted from built-up areas to the impervious surface area. Moreover, complex and multi-source indices were developed to increase accuracy. Most of the recent indices focus on enhancing the ISA and reducing bare soil and pervious surface areas.

There are numerous active RS sensors available and more currently under development. We divided these sections based on the spectral range of the bands. To simplify the discussion, we used the Landsat mission naming style instead of wavelength values.

Indices with Visible and Near-Infrared Bands

This section includes a few important urban spectral indices that used spectral bands ranging from 400–900 nm (see Table 1). Sensors with 400 to 900 nanometers (nm) of wavelength are the most common among earth imaging RS sensors. Satellite, airborne, and even unmanned aerial vehicles, almost all RS imaging sensors have this range of wavelength.

Usually, urban spectral indexing is popular with SWIR bands and early urban indices used at least one SWIR band. Estoque and Murayama (2015) argued that, besides urban built-up areas, dried vegetation also showed higher reflectance in the SWIR1 band region. Therefore, they proposed two built-up indices using visible bands only. They are visible red near-infrared built-up index (VrNIR-BI) and visible green near-infrared built-up index (VgNIR-BI). Among these two, VrNIR-BI works better than the VgNIR-BI index, and these are best in classifying ISA and dry vegetated areas, but not good at classifying ISA from bare soil.

Different versions of NDBI have been used to generate a newer binary built-up index (BBI) proposed using visible bands (Bai *et al.* 2020). Firstly, two binary NDBI indices $NDBI_{Blue\text{-}Green}$ and $NDBI_{Red\text{-}Green}$ calculated using the equation in Table 1. Secondly, BBI was calculated by adding all the positive binary values of those indices. Binary indices were indicated using the "b" at the subscript of the respective indices. Like NDBI (Zha *et al.* 2003), BBI does not distinguish between ISA and bare soil.

Another multi-indexed combinational biophysical composition index (CBCI) (Zhang *et al.* 2018) used two indices named modified bare soil index (MBSI) (Zhang *et al.* 2018) and optimized soil-adjusted vegetation index (OSAVI) (Moosavi *et al.* 2016; Rondeaux *et al.* 1996). MBSI is a soil index, and OSAVI is a vegetation index formulated as follows. Unlike BBI, CBCI has good separability between ISA and bare soil. In CBCI, "A" is a correctional factor that depends on soil characteristics, and its value is 0.51. "A" introduced to enhance MBSI over OSAVI. The strength of CBCI is that it can distinguish ISA when mixed with vegetation areas but is not quite good with soil areas.

Bai *et al.* (2020) also argued that removing waterbodies can significantly increase the ISA extraction accuracy. Like biophysical component index (BCI) and automated built-up extraction index, they proposed water extracted NDBI (WE-NDBI), which was formulated using multispectral *GF-1* wide-field view (WFV) sensor data sets. It required some logical functions to apply on $NDBI_{GF1}$ to keep those values only where water values are less than WE-NDVI. The study claimed that WE-NDBI significantly increases the accuracy in comparison to other NDBI indices. However, it does not separate bare soil from ISA.

Feature space is also popular with bare soil sensitive ISA indexing with visible bands and perpendicular indices. Tian *et al.* (2018) used feature spaces of blue and NIR bands to propose a reference line equation named perpendicular impervious surface index (PISI), which separates ISA from bare soil. Though using only two bands, it has higher accuracy in separating the impervious area from the bare soil area up to this point in time. PISI performed significantly better than the BCI and NDBI indices. It applies to most optical sensors due to the usage of blue and NIR bands only. The example of PISI can be replicated in numerous other RS applications. Similar to BBI, PISI increases the separability between ISA and bare soil and between ISA and vegetation areas.

Indices with Visible, NIR, and SWIR Bands

This section includes all the urban spectral indices that used visible, NIR, and SWIR bands. We exclude indices with PAN bands and include them in the following section (see Table 2). The first urban spectral index is named UI, proposed by Kawamura *et al.* (1997). A similar built-up index, which was the most used urban index, is the NDBI developed by Zha *et al.* (2003). Here, the authors attempted to develop a binary index using NDBI, where RSI will be classified as an urban and nonurban area. All positive NDBI values were considered as urban areas.

Despite the importance of distinguishing ISA from bare soil, innovative indices were developed slowly. For example, Jieli *et al.* (2010) worked on a new built-up index (NBI), which amplified built-up and bare land compared to NDBI. NBI is

Table 1. List of urban indices with spectral wavelength range 400–900 nm.

SL	Equation	EQN	Reference
1	$VrNIR-BI = (Red - NIR)/(Red + NIR)$	(1)	Estoque and Murayama 2015
2	$VgNIR-BI = (Green - NIR)/(Green + NIR)$	(2)	
3	$BBI = NDBI_{Blue-Green,b} + NDBI_{Red-Green,b}$ where, $NDBI_{Blue-Green} = (Blue - Green)/(Blue + Green)$, $NDBI_{Red-Green} = (Red - Green)/(Red + Green)$	(3)	Bai *et al.* 2020
4	$CBCI = (A+1) * MBSI - OSAVI + A$ where, $MBSI = ((Red + Green) * 2)/((Red + Green) - 2)$, $OSAVI = (NIR - RED)/(NIR + RED + 0.16)$ and $A = 0.51$	(4)	Zhang *et al.* 2018
5	$WE-NDBI = \begin{cases} NDBI_{GF1} (NDBI_{GF1} \le W) \\ 0 (NDBI_{GF1} > W) \end{cases}$ where, $NDBI_{GF1} = (Red - Green)/(Red + Green)$	(5)	Bai *et al.* 2020
6	$PISI = 0.8192 * Blue - 0.5735 * NIR + 0.0750$	(6)	Tian *et al.* 2018

SL = ; EQN = equation number.

producing an all positive urban index, but not as a normalized form. In NBI, the ordering of values is like bare land > built-up > other land classes from high to low. Using Landsat thematic mapper (TM) sensor data, a threshold value of 45–110 was used to extract the study's built-up area with 90% accuracy.

In pursuit of further development of NDBI, Waqar *et al.* (2012) proposed two new urban indices. They are normalized built-up area index (NBAI) and band ratio for the built-up area (BRBA). Here, NBAI used both of the SWIR regions where BRBA used only one SWIR band. The study claimed to increase built-up extraction accuracy by 10–13% compared to NDBI and NBI. All these indices could not separate the built-up areas from bare land areas.

Bouzekri *et al.* (2015) proposed a new built-up area extraction index based on *Landsat 8* and adding arithmetic constant in the nominator, where $L = 0.3$, is an arithmetic constant. To further enhance the urban land use classification accuracy, Kaimaris and Patias (2016) proposed a novel built-up index (BUI). Though innovative, BUI suffered from omission error. In BUI accuracy assessment, many built-up areas consider the non–built-up area. BUI also classified built-up and bare soil as one single class. Moreover, earlier urban researchers did not intend to differ between built-up and bare soil. NDBI never claimed to be an index of only urban rather than an indicator of the urban area showing built-up areas and bare lands.

Capolupo *et al.* (2020) used SWIR1 and red bands to introduce the SwiRed index. SWIR bands were the most used band regions in urban indexing practices. It is used to extract the built-up area in an automated land cover information extracting algorithm. Here, a threshold of $0 <$ value < 0.22 is used to classify built-up areas. SwiRed applies to temporal application with all the Landsat missions with SWIR bands.

Table 2. List of urban indices with spectral wavelength range 400–2500 nm excluding panchromatic (PAN) bands.

SL	Equation	EQN	Reference
1	$UI = \left((SWIR2 - NIR)/(SWIR2 + NIR) + 1\right) \times 100$	(7)	Kawamura *et al.* 1997
2	$NDBI = (SWIR1 - NIR)/(SWIR1 + NIR)$	(8)	Zha *et al.* 2003
3	$NBI = (Red \times SWIR1)/NIR$	(9)	Jieli *et al.* 2010
4	$NBAI = (SWIR2 - SWIR1/Green)/(SWIR2 + SWIR1/Green)$	(10)	Waqar *et al.* 2012
5	$BRBA = Red/SWIR1$	(11)	
6	$BAEI = (Red + L)/(Green + SWIR1)$	(12)	Bouzekri *et al.* 2015
7	$BUI = 2 * \frac{(Red * SWIR2) - (SWIR1 * SWIR2)}{(Red + SWIR1) * (SWIR1 + SWIR2)}$	(13)	Kaimaris and Patias 2016
8	$SwiRed = (SWIR1 - Red)/(SWIR1 + Red)$	(14)	Capolupo *et al.* 2020
9	$ENDISI = \frac{Blue - \alpha(SWIR1/SWIR2 + MNDWI^2)}{Blue + \alpha(SWIR1/SWIR2 + MNDWI^2)}$ where, $a = \frac{2 * Blue_{Mean}}{\left(\frac{SWIR1}{SWIR2}\right)_{Mean} + (MNDWI^2)_{Mean}}$	(15)	Chen *et al.* 2019
10	$BU_b = NDBI_b - NDVI_b$	(16)	Zha *et al.* 2003
11	$INDBI = NDBI - NDVI$, INDBI, also known as BUc	(17)	He *et al.* 2010
12	$IBI = \frac{[NDBI - (SAVI + MNDWI)/2]}{[NDBI + (SAVI + MNDWI)/2]}$	(18)	Xu 2008
13	$VIBI = NDVI/(NDVI - NDBI)$	(19)	Stathakis *et al.* 2012
14	$BCI = \frac{(H + L)/2 - V}{(H + L)/2 + V}$ where, H, V, and L are a normalized form of TC1, TC2, and TC3 bands	(20)	Deng and Wu 2012
15	$RNDSI = NNDSI/NTC1$, where, NNDSI is the normalized NDSI, and NTC1 is the normalized TC1	(21)	Deng *et al.* 2015
16	$CBI = \frac{(PC1 + NDWI)/2 - SAVI}{(PC1 + NDWI)/2 + SAVI}$ where, PC1 is the first band of PCA	(22)	Sun *et al.* 2016
17	$BLFEI = \frac{((Green + Red + SWIR2)/3) - SWIR1}{((Green + Red + SWIR2)/3) + SWIR1}$	(23)	Bouhennache *et al.* 2018

SL = ; EQN = equation number.

Chen *et al.* (2019) developed enhanced normalized difference impervious surface index (ENDISI) where preprocessing such as removing waterbodies is not required. Besides, it is efficient in separating bare soil from ISA. It used a generalized Gaussian model, and an automated threshold selection model for rapid IS extraction. ENDISI has one of the highest classification accuracies and can minimize background information, such as, bare soil, bare rock, and arid land significantly.

The urban area is inversely related to the vegetated area. Therefore, removing vegetated areas may enhance urban indexing accuracy. Following the principle, Zha *et al.* (2003) proposed a binary urban index (BU_b) where both NDBI and NDVI were transformed into a binary image based on whether they have positive value or not. Following that, He *et al.* (2010) modified it to another binary urban (BU_c) index where NDVI is subtracted from NDBI in its raw form. Later on, from the subtraction result, all positive value was transformed into one and negative values into zero. This BU_c is calculated from continuous value. Therefore, subscript c is used. BU_c is also named as an improved normalized difference built-up index (INDBI). INDBI performs 20% better than NDBI.

Similarly, another three indices-based index has been formulated and named as the index-based built-up index (IBI) (Xu 2008). Unlike NDBI, IBI tried to distinguish bare land from ISA. IBI used the green, red, NIR, and SWIR1 band region of Landsat TM/enhanced thematic mapper plus (ETM+). It used the combination of NDBI (Zha *et al.* 2003), soil adjusted vegetation index (SAVI) (Huete 1988), and the modified normalized difference water index (MNDWI) (Xu 2007) indices and output value ranging from −1 to +1. It slightly enhanced the ISA while suppressing other LULC classes (Langner *et al.* 2018). In the IBI-based LULC classification process, enhanced ISA has positive values and all other classes have a negative value. A similar zero threshold index was developed by Stathakis *et al.* (2012). However, the vegetation index built-up index (VIBI) has similarities with IBI and replicate the naming style of NDVI of Crippen (1990). This index used NDVI and NDBI as an element. It has a threshold of zero or very close to zero. It also made some improvement in separating ISA from bare soil. Authors claimed that VIBI has higher accuracy than other unsupervised classification though it suffers from the false-negative problem.

The spectral similarity of ISA and soil is a crucial problem that Deng and Wu (2012) first successfully addressed. The BCI is essential because of its ability to separate bare soil class from ISA. The authors proposed BCI based on the vegetation-impervious surface-soil (V-I-S) model (Ridd 2007) and using tasselled cap (TC) transformation (Kauth and Thomas 1976). BCI used the first three TC transformation to calculate the index. All the TC bands used in the equation were normalized beforehand. The benefit of using TC bands is that already various RS sensors have their TC coefficient developed. Therefore, BCI can be calculated from all these sensors besides Landsat. The removal of water bodies at the preprocessing stage allows the index to become more sensitive to bare soil and ISA difference. It can minimize bare soil because of its dry state.

Ratio normalized difference soil index (RNDSI) (Deng *et al.* 2015) suppressed every other feature class but bare soil. It used the first component of TC transformation (TC1) and normalized difference soil index (NDSI) (Rogers and Kearney 2010) to formulate RNDSI. RNDSI performed better than BCI and had high accuracy in separating ISA from bare soil. Similar indexing techniques were used by Sun *et al.* (2016) using PCA instead of TC to propose a combinational built-up index (CBI). It did not require the removal of water bodies. Instead of TC2 and TC3, it used vegetation index SAVI and NDWI. It is an improvement over BCI regarding dealing with water bodies. In BCI, waterbodies were required to remove prior calculation where CBI did not require the preprocessing steps.

On the contrary, Bouhennache *et al.* (2018) argued that the separability of built-up from bare soil could be achieved using SWIR1 and SWIR2 band spectral regions. They developed a built-up land features extraction index (BLFEI) using green, red, SWIR1, and SWIR2 operational land imager (OLI) bands. In BLFEI, water had the highest value and vegetation had the lowest. The values of impervious surface areas were lower than water and higher than bare soil areas. This index also had a higher spectral discrimination index than other similar urban indices.

Indices with PAN Band

All the urban indices with PAN bands are sensitive to the soil. Especially, ISA related indices are needed more to purify from pervious bare soil area. PAN band has a wide spectral range and usually is captured in higher spatial resolution.

Piyoosh and Ghosh (2017) modified the NDSI using a PAN band and named it "modified NDSI" (MNDSI). Where PAN is for panchromatic, MNDSI works better with bare bright soil. MNDSI also increases the spectral resolution slightly and provides better results than other soil indices. Piyoosh and Ghosh (2017) used BCI and MNDSI further and proposed a ratio of the urban index (RUI) (see Table 3). RUI increased the separability of bare soil and ISA.

Table 3. List of urban indices with panchromatic (PAN) bands.

SL	Equation	EQN	Reference
1	$\mathrm{MNDSI} = (\mathrm{SWIR2} - \mathrm{PAN})/(\mathrm{SWIR2} + \mathrm{PAN})$	(24)	Piyoosh and Ghosh 2017
2	$\mathrm{RUI} = \mathrm{BCI} / \mathrm{MNDSI}$	(25)	
3	$\mathrm{NRUI} = (\mathrm{RUI} - \mathrm{MNDSI})/(\mathrm{RUI} + \mathrm{MNDSI})$	(26)	

SL = ; EQN = equation number.

On the other hand, the normalized ratio of the urban index (NRUI) enhanced the separability even further. NRUI can distinguish soil and urban area better than RUI and BCI. Here, the author's method's novelty is to use the PAN band to calculate MNDSI, which increased the separability of ISA and bare soil area. Another advantage of the PAN band is pan-sharpening, which also increases LULC classification accuracy.

Indices with Thermal Bands

Urban artificial landscape often stores and emits more heat than surrounding nonurban areas, called the UHI phenomenon. Therefore, there is a spatial difference in temperature between urban and nonurban areas. Therefore, thermal RS data were used to developed newer spectral indices and increase classification accuracy. Normalized difference impervious surface index (NDISI), developed by Xu (2010), was the first automated index to deal with ISA which did not require removing water bodies and soil areas as preprocessing. It is also applicable to moderate resolution RS without the help of higher resolution images for manual assistance, where VIS_1 can be one of the visible bands. However, this index has some problems with water noise and is often mixed with ISA. To solve this problem, the authors suggested using a water index instead of visible bands.

Addressing that, various combinations of bands had been used in urban indexing. For example, As-syakur *et al.* (2012) included thermal, NIR, and SWIR1 bands for the new urban index development. Enhanced built-up and bareness index increase the separability among built-up and bare land and increase classification accuracy claimed in the study.

Furthermore, bare land areas also vary and not all of them are detectable using thermal band induced index, because in

urban areas, small-sized bare lands do not show any significant thermal variation (see Table 4).

A normalized difference water index (NDWI) or MNDWI can also be used as a water index in this equation. NDISI significantly increases the ISA signature, with a similar intention to enhance the ISA feature class and minimize the previous surface. Sun *et al.* (2017) proposed a modified NDISI ($MNDISI_{Sun}$) differently. Instead of the thermal infrared (TIR) band, the authors used the land surface temperature (LST) value. In this modification LST, or T_S, needs to be resampled to 30 m from TIR bands.

$MNDISI_{Sun}$ can be used for Landsat mission TM, ETM+, and OLI thermal infrared sensors (TIRS), but images from summertime will provide better results. With overall accuracy, 87% and an overall Kappa coefficient of 74%, $MNDISI_{Sun}$ is suitable for time series analysis with multiple Landsat missions. Another thermal data-based urban index, NDBI of Bhatti and Tripathi (2014), which is developed from the Landsat OLI data set and therefore renamed as $NDBI_{OLI}$, used PCA for formulation. In that study, the threshold value was selected through a double-window flexible pace search, increasing accuracy rather than traditional NDBI. $NDBI_{OLI}$ later helped develop another urban index named built-up area extraction method (BAEM) by Bhatti and Tripathi (2014).

Another example of multiple index-based urban indexes is BAEM. It is developed by Bhatti and Tripathi (2014) in an attempt to increase urban mapping accuracy. It is important to notice $NDBI_{OLI}$ (Bhatti and Tripathi 2014) is modified and calculated differently than what Zha *et al.* (2003) proposed. BAEM significantly improves the classification accuracy by reducing omission and commission errors.

The first NDBI-like ISA index was a normalized difference impervious index (NDII) developed using Landsat TM visual and thermal bands (Wang *et al.* 2015). In NDII, *Vis* stands for visible bands, and TIR stands for thermal bands. A combination of red band with a thermal band has found higher accuracy when tested with high-resolution images. NDII is a simple index and can be used for rapid ISA extraction using any multispectral data sets with thermal and visible bands. Urban ISA features have high correlations with thermal data and, conversely, vegetation has inverse correlations with urban ISA. In the next section, we discuss those urban indices those are using vegetation indices to formulate.

A thermal data set can be used to enhance classification accuracy. For example, Rasul *et al.* (2018) proposed a dry built-up index (DBI) using blue and thermal bands from Landsat OLI. DBI assumes that built-up areas have less vegetation and, therefore, low in NDVI values. Thus, subtracting NDVI can further enhance the built-up features. The study suggested using a threshold value of 0.72. Applicable in a dry climate, DBI has an overall classification accuracy of 93%. An urban area with high vegetation is not suitable to use DBI. Thermal data has some limitations to be considered before use. The spectral difference of thermal bands is mild and often shows phenological and daytime variation between urban and nonurban areas.

Indices with NTL RS

NTL RS is a night light sensor representing the human activity at night from space. The urban landscape is different in using light in contrast to nonurban areas. Therefore, using NTL spectral RS data with daytime, multispectral sensors have newer insights into urban studies (see Table 5).

In 2008, a multi-sourced human settlement index (HIS) fused Terra MODIS NDVI with an NTL data set, Defense Meteorological Satellite Program—Operational Linescan System (DMPS-OLS) (Lu *et al.* 2008). Both data sources have a coarse spatial resolution, but it serves well for large scale settlement mapping. $NDVI_m$ is the maximum NDVI derived from Terra MODIS, and NTL_N has a normalized DMSP-OLS data set into 0 to 1. Landsat ETM+ data set is used only as a reference in this index. With a larger pixel size, human settlement index (HSI) is a rapid and cost-effective indexing method, but it has a saturation problem.

Table 4. List of urban indices with thermal bands.

SL	Equation	EQN	Reference
1	$NDISI = \frac{TIR - (VIS_1 + NIR + SWIR1)/3}{TIR + (VIS_1 + NIR + SWIR1)/3}$	(27)	Xu 2010
2	$NDISI = \frac{TIR - (WI + NIR + SWIR1)/3}{TIR + (WI + NIR + SWIR1)/3}$	(28)	
3	$EBBI = \frac{SWIR1 + NIR}{10\sqrt{SWIR1 + TIR}}$	(29)	As-syakur *et al.* 2012
4	$MNDISI_{Sun} = \frac{T_S - (MNDWI + NIR + SWIR1)/3}{T_S + (MNDWI + NIR + SWIR1)/3}$; where, $T_S = \frac{TIR}{1 + \left(\frac{\lambda * TIR}{\rho}\right) ln\varepsilon}$, $\rho = 1.438 \times 10^{-2}$, $\varepsilon = \begin{cases} 0.979 - 0.035Red & NDVI < NDVI_{min} \\ 0.986 + 0.004P_V & NDVI_{min} < NDVI < NDVI_{max} \\ 0.99 & NDVI > NDVI_{max} \end{cases}$, $P_V = \left(\frac{NDVI - NDVI_{min}}{NDVI_{max} - NDVI_{min}}\right)^2$	(30)	Sun *et al.* 2017
5	$NDBI_{OLI} = \frac{(PCA\ of\ SWIR1, SWIR2 + PCA\ of\ TIR1, TIR2) - NIR}{(PCA\ of\ SWIR1, SWIR2 + PCA\ of\ TIR1, TIR2) - NIR}$	(31)	Bhatti and Tripathi 2014
6	$BAEM = NDBI_{OLI} - NDVI - MNDWI$	(32)	Bhatti and Tripathi 2014
7	$NDII = (Vis - TIR)/(Vis - TIR)$	(33)	Wang *et al.* 2015
8	$DBI = \frac{Blue - TIR1}{Blue + TIR1} - NDVI$	(34)	Rasul *et al.* 2018

SL = ; EQN = equation number.

Zhang *et al.* (2013) proposed the vegetation adjusted NTL urban index (VANUI) to solve the saturation problem. VANUI increases the NTL signal's contrast and better represents urban characteristics than previous NTL derived urban indices. It is useful for advanced urban studies, such as energy usage, carbon emissions, urban structures, etc. A similar approach with MODIS NDVI and the day/night band of visible infrared imaging radiometer suite's (VIIRS-DNB) adopts fractional ISA mapping. Guo *et al.* (2015) proposed a large-scale impervious surface index (LISI) that performs better than VANUI. Whereas $NDVI_{max}$ is the maximum annual MODIS NDVI and NTL_{nor} is the normalized NTL data of VIIRS-DNB. LISI has an overall accuracy of 0.13 and suitable for urban and rural area ISA mapping of a large area. At the same time, Zhang *et al.* (2015) similarly proposed a normalized difference urban index (NDUI). NDUI used Defense Meteorological Program Operational Line-Scan System (DMSP-OLS) and Landsat RSI. In this equation, NTL is the normalized DMSP-OLS image. Here, it is assumed that water has an NDVI value of less than 0 and the goal of the NDVI ≥ 0 part is dedicated to removing water pixels. With output value between 0 to 1, NDUI can separate mixed urban areas from bare lands and farmlands.

Another multi-sensor urban index used MODIS enhanced vegetation index (EVI), Landsat ETM+, and DMSP-OLS NTL data named normalized urban areas composite index (NUACI) contributed by increasing classification accuracy (Liu *et al.* 2015). It is calculated using three independent data sets: MODIS derived EVI, Landsat derived NDWI, and normalized DMSP-OLS image. This index also has a positive output value from 0 to 1. It eliminates the blooming effect and reduces saturation problems of coarse NTL data sets. Instead of coarse MODIS-based EVI (Huete *et al.* 1997), medium resolution Landsat-based SAVI (Qi *et al.* 1994) has been used in the formation of nighttime light adjusted impervious surface index (NAISI). Developed by Chen, Jia, and Pickering (2019) and followed by the baseline subtraction approach, NAISI used NTL, the first component of the principal component analysis (PC1), the third component of tasseled cap transformation (TC3), and SAVI. Here all the primary RS information is normalized before use. With the finer spatial resolution of NTL, this index can improve ISA extraction accuracy significantly.

In summary, the HSI used the MODIS NDVI and DMPS-OLS NTL data set (Lu *et al.* 2008). Later, using Landsat and NTL data, NDISI (MNDISILiu) modification was developed, which used thermal, NTL, and Landsat data sets (Liu *et al.* 2013). Afterward, MODIS EVI, Landsat ETM+, and DMSP-OLS were used to develop normalized urban areas composite index (NUACI) (Liu *et al.* 2015) with higher accuracy. On the other hand, VANUI correlates urban characteristics with vegetation absence and NTL presence (Zhang *et al.* 2013). A similar approach, normalized urban indexing, was later developed with NDUI (Zhang *et al.* 2015). All these indices discussed above use both NTL and daytime RSI. This combination can study many other global phenomena, especially with cloud computing platforms, such as GEE (Patel *et al.* 2015, Zhang *et al.* 2015). In the next section, we discuss urban indices with optical, NTL, and thermal data sets.

Complex Indices with Optical, NTL and Thermal Indices

Recently, few complex indices combined day and night RS data by using optical, thermal, and NTL data sets (see Table 6). Thermal RS data has been widely used in the UHI study. It has applications within urban spectral indexing too. In the previous section, optical and NTL data fusion has been shown at the pixel level. The added thermal data to formulate urban indices with higher accuracy were listed and discussed here.

Liu *et al.* (2013) modified NDISI (Xu 2010) and developed MNDISI, which address issues of spectral difference within IS and spectral similarity with other land cover classes, especially with bare soil. Here, T_{LST} is the daytime LST, L_{LIT} is the luminosity derived from nighttime light imagery, SAVI is the vegetation index, and SWIR1 is the band 5 in Landsat TM/ETM+ (Liu *et al.* 2013). $MNDISI_{Liu}$ is a multi-sourced index that used the three Rs data sets; ISS nighttime photograph, LST, and multispectral bands. Instead of ISS nighttime photograph, it can be calculated using the DMSP-OLS or VIIRS data set too. $MNDISI_{Liu}$ is useful for various scaled urban dynamics study with robust ISA extraction capacity. Another index named $MNDISI_{Sun}$ developed by Sun *et al.* (2017) is discussed in the previous section.

Similarly, Hao *et al.* (2015) also developed an index by combining optical, NTL, and thermal data. They used the NTL data set from DMSP-OLS, MODIS-based NDVI, and MODIS-based LST data while proposing VTLI. Here, $NDVI_{max}$ represents maximum annual NDVI, Tem_{max} represents the maximum annual night temperature, and NTL_{nor} represents normalized DMSP-OLS light data. All the data sets are normalized within 0 to 1.

Table 5. List of urban indices with nighttime lights (NTL) remote sensing (RS).

SL	Equation	EQN	Reference
1	$HSI = \frac{(1-NDVI_m)-NTL_N}{(1-NTL_N)+NDVI_m+(NDVI_m * NTL_N)}$	(35)	Lu *et al.* 2008
2	$VANUI = (1-NDVI_{nor}) * NTL_{nor}$	(36)	Zhang *et al.* 2013
3	$LISI = (1-NDVI_{max}) * \sqrt{NTL_{nor}}$	(37)	Guo *et al.* 2015
4	$NDUI = \frac{NTL-NDVI}{NTL+NDVI}, (NDVI \geq 0)$	(38)	Zhang *et al.* 2015
5	$NUACI = \begin{cases} 0. d > r, d = \sqrt{(NDWI-a)^2+(EVI_{max}-b)^2} \\ \left(1-\frac{d}{r}\right) * NTL_{Norm}, d \leq r \end{cases}$ where, d, r, and NTL_{norm} stands for the mean of NDWI, mean of EVI_{max}, and normalized form of DMSP-OLS image	(39)	Liu *et al.* 2015
6	$NAISI = \left(\frac{NTL-PC1_{nor}+TC3_{nor}}{2}\right)-SAVI_{nor}$	(40)	Chen *et al.* 2019

SL = ; EQN = equation number.

Table 6. List of complex urban indices.

SL	Equation	EQN	Reference
1	$MNDISI_{Liu} = \frac{T_{LST}+L_{LIT}-(SAVI+SWIR1)}{T_{LST}+L_{LIT}+(SAVI+SWIR1)}$	(41)	Liu *et al.* 2013
2	$VTLI = (1-NDVI_{max}) * Tem_{max} * NTL_{nor}$	(42)	Hao *et al.* 2015
3	$TVANUI = \frac{\arctan(LST/NDVI)}{\pi/2} * NTL$	(43)	Zhang *et al.* 2018

SL = ; EQN = equation number.

VTLI successfully enhanced DMSP-OLS data set by minimizing blooming and saturation effects. The study found that urban centers concentrated on 30% to 100% of high VTLI values. It is worth mentioning that VTLI uses a monthly composition data set from MODIS instead of daily data. It has both better accuracy and robustness than VANUI.

Furthermore, though it used a coarse MODIS data set, it achieved accuracy close to Landsat derived classification. Zhang and Li (2018) proposed temperature vegetation adjusted NTL urban index (TVANUI) using VI, NTL, and LST, which reduced the blooming and saturation effects of NTL. It was applied in both China and the U.S. and performed better than all earlier urban spectral indices. Inside TVANUI, all used indices are normalized. Negative values of NDVI consider 0 because, in negative NDVI, there is no ISA.

Discussion

In remote sensing, spectral indices are used for mapping, feature extraction, LULC, and similar studies. Multi-temporal scene-based studies can also deal with additional change detection studies (Chen *et al.* 2003; Gholinejad and Fatemi 2019). Furthermore, trend analysis and time series analysis is also popular with spectral indexing. All of the above mention studies have been applied in urban studies. Urban mapping (Thomas *et al.* 2003), urban change detection (Gupta and Munshi 2007), and urban time series analysis (Fu and Weng 2016) are more frequent.

Indexing Urban to ISA

In the beginning, urban researchers tried to index urbanism as a whole. Later urban characteristics, such as built-up areas, were emphasized in indices; for example, NDBI, NBAI, NBI, BUI are developed around the built-up nature of urban. Built-up areas are followed by imperviousness to being used in urban indexing. NDISI, NDII, ENDISI, MNDISI, LISI are all urban indices which index imperviousness in various ways.

Unlike the built-up area, ISA is a better indicator for the urban area. ISA used in urban characteristics, environmental issues, UHI, economic development, urban hydrology, urban flooding, etc. as an indicator. The problem with ISA is, by definition, it is the opposite of pervious bare soil. However, separating bare soil and ISA through spectral signature is very difficult. Therefore, separating these two classes are very crucial for recent urban indexing attempts.

Resolution Dependent Application

This section will discuss spatial, spectral, and temporal resolutions with their relation to indexing. We are omitting discussion of radiometric resolution because 8 bit resolution is enough for urban study and recent 14 bit sensors have no significant impact on urban studies.

Spatial Resolution

Urban areas tend to acquire smaller land use than other primary land covers. Midrange spatial resolutions, 10–30 meters, are enough to study urban mapping. A higher spatial resolution will provide better classification accuracy in solving the urban heterogeneity problem. On the contrary, airborne RS sensors have very high ground resolution and are applicable for detailed and more accurate LULC classification. The airborne platform can provide submeter spatial resolution along with detailing urban mapping capability.

Spectral Resolution

Multispectral RS has visible, NIR, SWIR, and TIR bands. All these bands are used in urban indexing. Among them, SWIR is most used and followed by NIR for urban indexing.

Multispectral RS has spectral limitations and many of them can be solved by adopting hyperspectral RSI. NTL has a coarser spectral range, ranging from 400–1000 nm in DMSP-OLS and 500–900 nm in *Suomi-NPP*. Hyperspectral RS is unique for its equal spaced spectral ranges. Spectral ranges and the number of bands vary per sensor. The study of spectral signature is a by-product of hyperspectral RS and help detail LULC classification.

Temporal Resolution

Single cloud-free RSI is enough for urban mapping, but cloud coverage is a common problem in optical RS and often requires extracting cloud-free pixels from multiple RSI. In this case, higher temporal resolution plays a good role. Change detection studies required fair temporal resolution based on the duration of the study. Time series analysis, on the contrary, needs flexible temporal data availability to conduct. Recently, monthly image-based time-series studies are getting popular, which requires very high temporal resolution. Furthermore, RSI composites are getting trendy in mapping to time series analysis.

Sensor Dependent Application

Sensor types also have an impact on urban indexing. Optical, thermal, and NTL sensors all have pixel format in data storage, therefore useable together. Furthermore, most of the urban spectral indices are developed from optical multispectral RS have NIR and SWIR bands, which are the primary bands used for urban spectral indexing. Urban ISA has high reflectance in the SWIR spectral region and medium reflectance in the NIR spectral region. Earlier urban indices were developed using these two spectral regions.

Urban ISA is hotter than the surrounding environment due to UHI phenomena. Many urban studies also used thermal characteristics to develop better urban spectral indices. Based on that, $NDBI_{OLI}$ (Bhatti and Tripathi 2014), NDII (Wang *et al.* 2015), NDISI (Xu 2010), $MNDISI_{Sun}$ (Sun *et al.* 2017), DBI (Rasul *et al.* 2018), and TVANUI (Zhang and Li 2018) are some of the examples of the thermal band used in urban spectral indexing. Thermal bands are usually coarser than optical bands and it is a limitation of NTL sensors. Furthermore, seasonality and time of the day affect the thermal bands' separability.

NTL is very popular among RS researchers and unbiasedly presents human activity from space through light. Every type of NTL data does not represent urban lights; only temporally stable NTL's do. Therefore, normalized stable NTL data is often used for urban indexing purposes. Regional mapping is preferable with NTL because of its coarse spatial resolution where either it overlooks or overestimates smaller settlements in single city studies with NTL. Last of all, data limitations, saturation, and blooming effects are some of the limitations which are minimized in newer NTL's.

Spectral Confusion Between ISA and Bare Soil

Urban ISA and bare soil are the two most confusing LULC classes in the optical RS domain. Spectral similarity, chemical composition, and even visible color are so similar that the earliest urban indices consider them as one class. To this end, the problem of spectral similarity can be solved using hyperspectral RS, tasseled cap transformation, panchromatic band, and so on. Deng and Wu (2012) used tasseled cap transformations to develop BCI, which has good separability of ISA and bare soil with mild contrast. Piyoosh and Ghosh (2017) developed MNDSI using PAN bands.

Nevertheless, not all sensors have PAN bands. Therefore, Bouhennache *et al.* (2018) developed BLFEI without using PAN bands. All these indices are capable of distinguishing ISA and bare soil. Another approach to estimating ISA is to subtract bare soil from it. For instance, Rasul *et al.* (2018) developed the dry bare-soil index and the urban index DBI.

Moreover, thermal bands and NTL information is also useful to separate urban ISA from bare soil. Finally, thermal data's potential limitation is the difference between these two data,

which is mild and varies seasonally. In the case of NTL, it has a very coarse spatial resolution.

Threshold

Image segmentation with indexing requires thresholds. Usually, researchers use their experience and trial and error techniques to define a more accurate threshold for a particular study, which works fine with their selected study time, place, and data sets. However, the threshold often varies spatiotemporally. Following that, automatic thresholding can speed up the segmentation process. With urban ISA extraction, the accurate threshold is crucial (Firozjaei *et al.* 2019), such as the OTSU method, but it works better on well distinguishable two classes. Hence, it is not recommended with multiclass classification.

Limitations

Our work has several limitations. Firstly, we list urban indices and discuss their merits and demerits, but did not perform any comparative analysis. However, we cite some previous comparative work. Secondly, we enlisted urban spectral indices but did not suggest any ranking for them. However, we discussed the performance between the two indices in some instances. Thirdly, we have not discussed the development process of those indices. Besides, choosing one or more urban indices depends on the study's circumstances.

Fourthly, we did not include any index with hyperspectral, LiDAR, and synthetic aperture radar (SAR) RS data. Hyperspectral RS data has enormous potentials in urban studies with indices, especially in classifying ISA from bare soil class and addressing urban heterogeneity (Zhu *et al.* 2019). Besides hyperspectral, SAR and LiDAR data sets are also helpful in the vertical study of urban spaces. Detecting urban vertical expansion is difficult to measure with optical RS but LiDAR and SAR can be useful for these purposes and can be fused at the decision level to get better classification results.

Finally, we mention only the OTSU method in the threshold subsection, but many other thresholding techniques are not discussed here. Moreover, the selection of thresholding techniques might also vary per index. Further studies may work on thresholding and spectral indices in the future.

Knowledge Gaps

In the last two decades, spectral urban studies experienced many developments, but many questions remain unanswered. We are yet to know the common spectral urban characteristics that function globally. Although NTL data has some potential in this case further study is required. We do not know yet how to define an urban area from RSI, irrespective of geographical difference. Besides, there is an absence of common global characteristics of the urban area since urban areas are highly heterogeneous. Not only spatially but also temporally, phenology affects LULC classification (Wang and Li 2019). For the time being, the most common problem is the spectral similarity of bare soil and ISA. Above all, these are the few questions that need to be answered to advance the future urban RS domain.

The term urban is vague and differs administratively in parallel with infrastructural importance, population size, economic value, and political status. All these factors influence defining the term urban. However, in RS studies, there is no perfect spectral index to define urban areas. Thereupon, it can function only as an indicator.

Future Direction

The fusion of multiple RS source types is trending now. Sooner or later, more multi-source spectral indices will be developed. Spectrally, hyperspectral RS data have substantial potential solving LULC classification problems. Besides, NTL is also a very popular nighttime RS that can easily depict night scenes from space, even though coarse spatial resolution is limiting its application in urban studies. Newer and improved NTL sensors also have high potentials in advanced urban indexing.

Active RS sensors, such as SAR and LiDAR have advantages in urban studies. These sensors can function both day and night, penetrate clouds, and fog and mist are measured by vertical changes. Though these sensors are different from spectral sensors, innovative fusing techniques can still be used in urban studies. Already, fusing Landsat and SAR data sets were used to estimate ISA and separate ISA from bare soil (Yang *et al.* 2009). Besides, LiDAR has the potential for measuring vertical urban changes.

Zhu *et al.* (2019) reviewed four strategic directions for urban RS studies. These directions are based on higher temporal resolution, hyperspectral remote imagery (HRI), fusing multiple RS data sets, and combining RS data with structural and nonstructural data. Among these four directions, HRI and multiple RS source fusion are directly linked with spectral indexing.

The first urban index was related to population density. Besides population density, GIS data such as population, temperature, rainfall, gross domestic product, traffic, transport details, energy usage, etc., also have potentials in newer urban indexing.

The use of cloud platforms like GEE and free RS data sources will increase indices' use. Apart from that, GEE has global mapping and time-series visualization features. It also has data available from the mid-'90s or even before. Henceforth, future developments may adopt spectral index-based LULC measurements along with it.

In addition, along with the study of urban physical characteristics, soon many abstract issues will be studied assisted with RS spectral indices. Abstract urban concepts, such as seasonality, sustainability, biodiversity, livability, green city, walkability, happiness, richness, urbanism, and so on can be studied using RS spectral indices.

Conclusions

Here, we summarize all the important spectral urban indices with their equations, advantages, and disadvantages and classify them based on their band requirements.

We found that instead of inefficiency, the earlier developed urban spectral indices were simple, single-sourced, and robust to use. Conversely, recent indices are complex, multi-sourced, sophisticated, use rare spectral bands, and are more accurate. Actually, urban indexing began with mapping urban area as a whole and later became more specific in mapping urban characteristics. However, newer RS data sources are becoming available every year with improved capacity and features. The demand for better measurement is now forcing RS researchers to search for improved indices. Cloud computing platforms like GEE and enhanced computing capacity allowed researchers to build complex indices. In addition, overcoming spatiotemporal barriers requires more robust indices. To conclude, the future of urban indexing will determine how efficiently we can answer those questions.

Acknowledgments

The authors are sincerely grateful to the editors and anonymous reviewers for their valuable suggestions and comments that significantly improved this paper. This work is supported by the National Key Research and Development Program of China (2018YFB0505401), the Research Project from the Ministry of Natural Resources of China under Grant 4201-240100123, the National Natural Science Foundation of China under Grants 41771452, 41771454, 41890820, and 41901340,

the Natural Science Fund of Hubei Province in China under Grant 2018CFA007, the Natural Science Foundation of Inner Mongolia Autonomous Region (2019MS04017), and the Scientific research project of colleges and universities in Inner Mongolia Autonomous Region (NJZY20277).

References

As-syakur, A. R., I.W.S. Adnyana, I. W. Arthana and I. W. Nuarsa. 2012. Enhanced built-up and bareness index (EBBI) for mapping built-up and bare land in an urban area. *Remote Sensing* 4(10):2957–2970.

Bai, Y., G. He, G. Wang and G. Yang. 2020. WE-NDBI—A new index for mapping urban built-up areas from GF-1 WFV images. *Remote Sensing Letters* 11(5):407–415.

Baret, F., G. Guyot and D. Major. 1989. TSAVI: A vegetation index which minimizes soil brightness effects on LAI and APAR estimation. Pages 1355–1358 in *Proceedings of the 12th IEEE Canadian Symposium on Remote Sensing Geoscience and Remote Sensing Symposium*, held in Vancouver, Canada.

Bhatti, S. S. and N. K. Tripathi. 2014. Built-up area extraction using Landsat 8 OLI imagery. *GIScience Remote Sensing* 51(4):445–467.

Bouhennache, R., T. Bouden, A. Taleb-Ahmed and A. Cheddad. 2018. A new spectral index for the extraction of built-up land features from Landsat 8 satellite imagery. *Geocarto International* 34(14):1531–1551.

Bouzekri, S., A. A. Lasbet and A. Lachehab. 2015. A new spectral index for extraction of built-up area using Landsat-8 data. *Journal of the Indian Society of Remote Sensing* 43(4):867–873.

Capolupo, A., C. Monterisi and E. Tarantino. 2020. Landsat images classification algorithm (LICA) to automatically extract land cover information in Google earth engine environment. *Remote Sensing* 12(7):28.

Chen, J., P. Gong, C. He, R. Pu and P. Shi. 2003. Land-use/land-cover change detection using improved change-vector analysis. *Photogrammetric Engineering & Remote Sensing* 69(4):369–379.

Chen, J., K. Yang, S. Chen, C. Yang, S. Zhang and L. He. 2019. Enhanced normalized difference index for impervious surface area estimation at the plateau basin scale. *Journal of Applied Remote Sensing* 13(01):19.

Chen, X., X. Jia and M. Pickering. 2019. A nighttime lights adjusted impervious surface index (NAISI) with integration of Landsat imagery and nighttime lights data from international space station. *International Journal of Applied Earth Observation and Geoinformation*:83.

Chikr El-Mezouar, M. 2011. Vegetation extraction from IKONOS imagery using high spatial resolution index. *Journal of Applied Remote Sensing* 5(1):14.

Colwell, J. E. 1974. Vegetation canopy reflectance. *Remote Sensing of Environment* 3(3):175–183.

Crippen, R. E. 1990. Calculating the vegetation index faster. *Remote Sensing of Environment* 34 (1):71–73.

Datta, R., D. Joshi, J. Li and J. Wang. 2008. Image retrieval: Ideas, influences, and trends of the new age. *ACM Computing Surveys* 40(2):1–60.

Dekker, A. G., T. J. Malthus, M. M. Wijnen and E. Seyhan. 1992. The effect of spectral bandwidth and positioning on the spectral signature analysis of inland waters. *Remote Sensing of Environment* 41(2–3):211–225.

Deng, C. and C. Wu. 2012. BCI: A biophysical composition index for remote sensing of urban environments. *Remote Sensing of Environment* 127:247–259.

Deng, Y., C. Wu, M. Li and R. Chen. 2015. RNDSI: A ratio normalized difference soil index for remote sensing of urban/suburban environments. *International Journal of Applied Earth Observation and Geoinformation* 39:40–48.

Digirolamo, L. and R. Davies. 1994. A band-differenced angular signature technique for cirrus cloud detection. *IEEE Transactions on Geoscience and Remote Sensing* 32(4):890–896.

Duan, Y., X. Shao, Y. Shi, H. Miyazaki, K. Iwao and R. Shibasaki. 2015. Unsupervised global urban area mapping via automatic labeling from ASTER and PALSAR satellite images. *Remote Sensing* 7(2):2171–2192.

Estoque, R. C. and Y. Murayama. 2015. Classification and change detection of built-up lands from Landsat-7 ETM+ and Landsat-8 OLI/TIRS imageries: A comparative assessment of various spectral indices. *Ecological Indicators* 56:205–217.

Firozjaei, M., A. Sedighi, M. Kiavarz, S. Qureshi, D. Haase and S. Alavipanah. 2019. Automated built-up extraction index: A new technique for mapping surface built-up areas using LANDSAT 8 OLI imagery. *Remote Sensing* 11(17):20.

Fu, P. and Q. H. Weng. 2016. A time series analysis of urbanization induced land. use and land cover change and its impact on land surface temperature with Landsat imagery. *Remote Sensing of Environment* 175:205–214.

Gholinejad, S. and S. B. Fatemi. 2019. Optimum indices for vegetation cover change detection in the Zayandeh-rud river basin: A fusion approach. *International Journal of Image and Data Fusion* 10(3):199–216.

Gomez-Chova, L., J. Amoros-Lopez, G. Mateo-Garcia, J. Munoz-Mari and G. Camps-Valls. 2017. Cloud masking and removal in remote sensing image time series. *Journal of Applied Remote Sensing*:11.

Gorelick, N., M. Hancher, M. Dixon, S. Ilyushchenko, D. Thau and R. Moore. 2017. Google Earth engine: Planetary-scale geospatial analysis for everyone. *Remote Sensing of Environment* 202:18–27.

Guo, W., D. Lu, Y. Wu and J. Zhang. 2015. Mapping impervious surface distribution with integration of SNNP VIIRS-DNB and MODIS NDVI data. *Remote Sensing* 7(9):12459–12477.

Gupta, D. M. and M. K. Munshi. 2007. Urban change detection and land-use mapping of Delhi. *International Journal of Remote Sensing* 6(3-4):529–534.

Hao, R., D. Yu, Y. Sun, Q. Cao, Y. Liu and Y. Liu. 2015. Integrating multiple source data to enhance variation and weaken the blooming effect of DMSP-OLS light. *Remote Sensing* 7(2):1422–1440.

He, C., P. Shi, D. Xie and Y. Zhao. 2010. Improving the normalized difference built-up index to map urban built-up areas using a semiautomatic segmentation approach. *Remote Sensing Letters* 1(4):213–221.

Hester, D. B., S.A.C. Nelson, H. I. Cakir, S. Khorram and H. Cheshire. 2010. High-resolution land cover change detection based on fuzzy uncertainty analysis and change reasoning. *International Journal of Remote Sensing* 31(2):455–475.

Howarth, P. J. and E. Boasson. 1983. Landsat digital enhancements for change detection in urban environments. *Remote Sensing of Environment* 13(2):149–160.

Huete, A., H. Liu, K. Batchily and W. Van Leeuwen. 1997. A comparison of vegetation indices over a global set of TM images for EOS-MODIS. *Remote Sensing of Environment* 59(3):440–451.

Huete, A. R. 1988. A soil-adjusted vegetation index (SAVI). *Remote Sensing of Environment* 25(3):295–309.

Jawak, S. D. and A. J. Luis. 2013. Improved land cover mapping using high resolution multiangle 8-band WorldView-2 satellite remote sensing data. *Journal of Applied Remote Sensing* 7(1):21.

Jieli, C., L. Manchun, L. Yongxue, S. Chenglei and H. Wei. 2010. Extract residential areas automatically by new built-up index. Pages 1–5 in Proceedings of the 2010 18th *IEEE International Conference on Geoinformatics*, held in Beijing, China.

Kaimaris, D. and P. Patias. 2016. Identification and area measurement of the built-up area with the built-up index (BUI). *International Journal of Advanced Remote Sensing and GIS* 5(1):1844–1858.

Kauth, R. J. and G. S. Thomas. 1976. The tasselled cap—A graphic description of the spectral-temporal development of agricultural crops as seen by LANDSAT. In *IEEE Symposium on Machine Processing of Remotely Sensed Data*, West Lafayette, Indiana: Purdue University.

Kawamura, M., S. Jayamanna and Y. Tsujiko. 1997. Quantitative evaluation of urbanization in developing countries using satellite data. *Doboku Gakkai Ronbunshu* 1997(580):45–54.

Khan, A., S. Chatterjee, H. Akbari, S. Bhatti, A. Dinda, C. Mitra, H. Hong and Q.-V. Doan. 2017. Step-wise land-class elimination approach for extracting mixed-type built-up areas of Kolkata megacity. *Geocarto International*:1–47.

Kobayashi, N., H. Tani, X. Wang and R. Sonobe. 2019. Crop classification using spectral indices derived from Sentinel-2A imagery. *Journal of Information and Telecommunication* 4(1):67–90.

Langner, A., J. Miettinen, M. Kukkonen, C. Vancutsem, D. Simonetti, G. Vieilledent, A. Verhegghen, J. Gallego and H.-J. Stibig. 2018. Towards operational monitoring of forest canopy disturbance in evergreen rain forests: A test case in continental southeast Asia. *Remote Sensing* 10(4).

Li, C., Shao, Z., Zhang, L., Huang, X. and Zhang, M., 2021. A Comparative Analysis of Index-Based Methods for Impervious Surface Mapping Using Multiseasonal Sentinel-2 Satellite Data, *IEEE Journal of Selected Topics in Applied Earth Observations and Remote Sensing*, 14:3682-3694.

Li, D., Ma, J., Cheng, T., van Genderen, J.L. and Shao, Z., 2018. Challenges and opportunities for the development of megacities, *International Journal of Digital Earth*.

Li, W. 2020. Mapping urban impervious surfaces by using spectral mixture analysis and spectral indices. *Journal of Remote Sensing* 12(1):94.

Liu, C., Z. Shao, M. Chen and H. Luo. 2013. MNDISI: A multi-source composition index for impervious surface area estimation at the individual city scale. *Remote Sensing Letters* 4(8):803–812.

Liu, J. and P. Li. 2019. Extraction of earthquake-induced collapsed buildings from bi-temporal VHR images using object-level homogeneity index and histogram. *IEEE Journal of Selected Topics in Applied Earth Observations and Remote Sensing* 12(8):2755–2770.

Liu, X., G. Hu, B. Ai, X. Li and Q. Shi. 2015. A normalized urban areas composite index (NUACI) based on combination of DMSP-OLS and MODIS for mapping impervious surface area. *Remote Sensing* 7(12):17168–17189.

Liu, X., G. Hu, Y. Chen, X. Li, X. Xu, S. Li, F. Pei and S. Wang. 2018. High-resolution multi-temporal mapping of global urban land using Landsat images based on the Google Earth engine platform. *Remote Sensing of Environment* 209:227–239.

Lu, D., H. Tian, G. Zhou and H. Ge. 2008. Regional mapping of human settlements in southeastern China with multisensor remotely sensed data. *Remote Sensing of Environment* 112(9):3668–3679.

Meyer, W. B. and B. L. Turner II, eds. 1994. *Changes in Land Use and Land Cover: A Global Perspective*. Cambridge, United Kingdom: Cambridge University Press.

Lyimo, N.N., Shao, Z., Ally, A.M., Twumasi, N.Y.D., Altan, O. and Sanga, C.A., 2020. A Fuzzy Logic-Based Approach for Modelling Uncertainty in Open Geospatial Data on Landfill Suitability Analysis, *ISPRS International Journal of Geo-Information*, 9(12):737.

Moosavi, V., A. Talebi, M. H. Mokhtari and M. R. Hadian. 2016. Estimation of spatially enhanced soil moisture combining remote sensing and artificial intelligence approaches. *International Journal of Remote Sensing* 37(23):5605–5631.

Nichol, J. and C. M. Lee. 2006. Urban vegetation monitoring in Hong Kong using high resolution multispectral images. *International Journal of Remote Sensing* 26(5):903–918.

Nouri, H., S. Beecham, S. Anderson and P. Nagler. 2014. High spatial resolution WorldView-2 imagery for mapping NDVI and its relationship to temporal urban landscape evapotranspiration factors. *Remote Sensing* 6(1):580–602.

Olaode, A., G. Naghdy and C. Todd. 2014. Unsupervised classification of images: A review. *International Journal of Image Processing* 8(5):325–342.

Pan, X.-Z., S. Uchida, Y. Liang, A. Hirano and B. Sun. 2010. Discriminating different landuse types by using multitemporal NDXI in a rice planting area. *International Journal of Remote Sensing* 31(3):585–596.

Parent, J. R., J. C. Volin and D. L. Civco. 2015. A fully-automated approach to land cover mapping with airborne LiDAR and high resolution multispectral imagery in a forested suburban landscape. *ISPRS Journal of Photogrammetry and Remote Sensing* 104:18–29.

Patel, N. N., E. Angiuli, P. Gamba, A. Gaughan, G. Lisini, F. R. Stevens, A. J. Tatem and G. Trianni. 2015. Multitemporal settlement and population mapping from Landsat using Google Earth engine. *International Journal of Applied Earth Observation and Geoinformation* 35:199–208.

Phalke, A. R. and M. Özdoğan. 2018. Large area cropland extent mapping with Landsat data and a generalized classifier. *Remote Sensing of Environment* 219:180–195.

Piyoosh, A. K. and S. K. Ghosh. 2017. Development of a modified bare soil and urban index for Landsat 8 satellite data. *Geocarto International* 33(4):423–442.

Qi, J., A. Chehbouni, A. R. Huete, Y. H. Kerr and S. Sorooshian. 1994. A modified soil adjusted vegetation index. *Remote Sensing of Environment* 48(2):119–126.

Qin, R. and W. Fang. 2014. A hierarchical building detection method for very high resolution remotely sensed images combined with DSM using graph cut optimization. *Photogrammetric Engineering & Remote Sensing* 80(9):873–883.

Rasul, A., H. Balzter, G. Ibrahim, H. Hameed, J. Wheeler, B. Adamu, S.a. Ibrahim and P. Najmaddin. 2018. Applying built-up and bare-soil indices from Landsat 8 to cities in dry climates. *Land* 7(3).

Ridd, M. K. 2007. Exploring a V-I-S (vegetation-impervious surface-soil) model for urban ecosystem analysis through remote sensing: Comparative anatomy for cities. *International Journal of Remote Sensing* 16(12):2165–2185.

Rogers, A. S. and M. S. Kearney. 2010. Reducing signature variability in unmixing coastal marsh Thematic Mapper scenes using spectral indices. *International Journal of Remote Sensing* 25(12):2317–2335.

Rondeaux, G., M. Steven and F. Baret. 1996. Optimization of soil-adjusted vegetation indices. *Remote Sensing of Environment* 55(2):95–107.

Rouse Jr, J. W., R. Haas, J. Schell and D. Deering. 1974. Monitoring vegetation systems in the Great Plains with ERTS. Pages 301–317 in Proceedings of the *Third Earth Resources Technology Satellite-1 Symposium*, Volume I: Technical Presentations. NASA SP-351. Edited by S. C. Freden, E. P. Mercanti, and M. A. Becker. Wash., D.C.: NASA.

Sellers, P. 1987. Canopy reflectance, photosynthesis, and transpiration, II. The role of biophysics in the linearity of their interdependence. *Remote Sensing of Environment* 21(2):143–183.

Shao, Z., Wu, W. and Li, D., 2021. Spatio-temporal-spectral observation model for urban remote sensing, *Geo-Spatial Information Science*:1-15.

Shao, Z.F., Fu, H.Y., Li, D.R., Altan, O. and Cheng, T., 2019. Remote sensing monitoring of multi-scale watersheds impermeability for urban hydrological evaluation, *Remote Sensing of Environment*, 232:11.

Shelestov, A., M. Lavreniuk, N. Kussul, A. Novikov and S. Skakun. 2017. Exploring Google Earth engine platform for big data processing: classification of multi-temporal satellite imagery for crop mapping. *Frontiers in Earth Science* 5:1–10.

Stathakis, D., K. Perakis and I. Savin. 2012. Efficient segmentation of urban areas by the VIBI. *International Journal of Remote Sensing* 33(20):6361–6377.

Sun, G., X. Chen, X. Jia, Y. Yao and Z. Wang. 2016. Combinational build-up index (CBI) for effective impervious surface mapping in urban areas. *IEEE Journal of Selected Topics in Applied Earth Observations and Remote Sensing* 9(5):2081–2092.

Sun, Z., C. Wang, H. Guo and R. Shang. 2017. A modified normalized difference impervious surface index (MNDISI) for automatic urban mapping from landsat imagery. *Remote Sensing* 9(9):18.

Surin, V. G. and G. A. Ladner. 1995. Spectral signatures of vegetation in the 8-to-14 mu-m thermal infrared region. *Earth Observation and Remote Sensing* 12(3):341–352.

Thomas, N., C. Hendrix and R. G. Congalton. 2003. A comparison of urban mapping methods using high-resolution digital imagery. *Photogrammetric Engineering and Remote Sensing* 69(9):963–972.

Tian, Y., H. Chen, Q. Song and K. Zheng. 2018. A novel index for impervious surface area mapping: development and validation. *Remote Sensing* 10(10):23.

Vachon, P. W. and J. C. West. 1992. Spectral estimation techniques for multilook SAR images of ocean waves. *IEEE Transactions on Geoscience and Remote Sensing* 30(3):568–577.

Wang, Y. and M. Li. 2019. Urban impervious surface detection from remote sensing images: A review of the methods and challenges. *IEEE Geoscience and Remote Sensing Magazine* 7(3):64–93.

Wang, Z., C. Gang, X. Li, Y. Chen and J. Li. 2015. Application of a normalized difference impervious index (NDII) to extract urban impervious surface features based on Landsat TM images. *International Journal of Remote Sensing* 36(4):1055–1069.

Waqar, M. M., J. F. Mirza, R. Mumtaz and E. Hussain. 2012. Development of new indices for extraction of built-up area & bare soil from Landsat data. *Open Access Scientific Reports* 1(1):4.

Wu, W., Q. Li, Y. Zhang, X. Du and H. Wang. 2018. Two-step urban water index (TSUWI): A new technique for high-resolution mapping of urban surface water. *Remote Sensing* 10(11):21.

Xie, Y., Z. Sha and M. Yu. 2008. Remote sensing imagery in vegetation mapping: A review. *Journal of Plant Ecology* 1(1):9–23.

Xu, H. 2007. Modification of normalised difference water index (NDWI) to enhance open water features in remotely sensed imagery. *International Journal of Remote Sensing* 27(14):3025–3033.

Xu, H. 2008. A new index for delineating built-up land features in satellite imagery. *International Journal of Remote Sensing* 29(14):4269–4276.

Xu, H. 2010. Analysis of impervious surface and its impact on urban heat environment using the normalized difference impervious surface index (NDISI). *Photogrammetric Engineering & Remote Sensing* 76(5):557–565.

Xue, J. and B. Su. 2017. Significant remote sensing vegetation indices: A review of developments and applications. *Journal of Sensors* 2017:1–17.

Yang, L., L. Jiang, H. Lin and M. Liao. 2009. Quantifying sub-pixel urban impervious surface through fusion of optical and in SAR imagery. *GIScience & Remote Sensing* 46(2):161–171.

Zha, Y., J. Gao and S. Ni. 2003. Use of normalized difference built-up index in automatically mapping urban areas from TM imagery. *International Journal of Remote Sensing* 24(3):583–594.

Zhang, Q., C. Schaaf and K. C. Seto. 2013. The vegetation adjusted NTL urban index: A new approach to reduce saturation and increase variation in nighttime luminosity. *Remote Sensing of Environment* 129:32–41.

Zhang, Q. and K. C. Seto. 2011. Mapping urbanization dynamics at regional and global scales using multi-temporal DMSP/OLS nighttime light data. *Remote Sensing of Environment* 115(9):2320–2329.

Zhang, Q., B. Li, D. Thau and R. Moore. 2015. Building a better urban picture: Combining day and night remote sensing imagery. *Remote Sensing* 7(9):11887–11913.

Zhang, S., K. Yang, M. Li, Y. Ma and M. Sun. 2018. Combinational biophysical composition index (CBCI) for effective mapping biophysical composition in urban areas. *IEEE Access* 6:41224–41237.

Zhang, X. and P. Li. 2018. A temperature and vegetation adjusted NTL urban index for urban area mapping and analysis. *ISPRS Journal of Photogrammetry and Remote Sensing* 135:93–111.

Zhang, Y. and Shao, Z., 2021. Assessing of Urban Vegetation Biomass in Combination with LiDAR and High-resolution Remote Sensing Images, *International Journal of Remote Sensing*, 42(3):964-985.

Zhu, Z., Y. Zhou, K. C. Seto, E. C. Stokes, C. Deng, S. T. Pickett and H. Taubenböck. 2019. Understanding an urbanizing planet: Strategic directions for remote sensing. *Remote Sensing of Environment* 228:164–182.